Interaction and control of a human-exoskeleton system

Aurélie Bonnefoy, Sabrina Otmani, Nicolas Mansard, Olivier Stasse, Guilhem Michon, Bruno Watier

▶ **To cite this version:**

Aurélie Bonnefoy, Sabrina Otmani, Nicolas Mansard, Olivier Stasse, Guilhem Michon, et al.. Interaction and control of a human-exoskeleton system. 2023 International Symposium on Medical Robotics (ISMR), Apr 2023, Atlanta, United States. pp.1-7, ⟨10.1109/ISMR57123.2023.10130232⟩. ⟨hal-04942985⟩

HAL Id: hal-04942985

https://laas.hal.science/hal-04942985v1

Submitted on 12 Feb 2025

HAL is a multi-disciplinary open access archive for the deposit and dissemination of scientific research documents, whether they are published or not. The documents may come from teaching and research institutions in France or abroad, or from public or private research centers.

L'archive ouverte pluridisciplinaire **HAL**, est destinée au dépôt et à la diffusion de documents scientifiques de niveau recherche, publiés ou non, émanant des établissements d'enseignement et de recherche français ou étrangers, des laboratoires publics ou privés.

Distributed under a Creative Commons CC0 1.0 - Universal - International License

Interaction and control of a human-exoskeleton system.

Sabrina OTMANI[1,2], Aurélie BONNEFOY[2], Guilhem MICHON[1],
Olivier STASSE[2], Nicolas MANSARD[2], Bruno WATIER[2]

***Abstract*— This paper presents a way to control an exoskeleton for patient suffering from stroke cerebral palsy (CP). More precisely a model of the gait related to CP type-C is proposed and corrected through a whole body QP-controller. The model is be done using mechanical differential equations, while the whole body QP controller is implemented through a Weighted Quadratic Program (WQP) called TSID. A unique feature of this paper is the Clinical Gait Analysis (CGA) and EMG acquisitions performed on two 9 years old twin sisters. One has spastic cerebral palsy (C) while the other is healthy (H) thus without any impairment. This paper aims to correct the gait of C and converge to the one of H. The interaction between the human and the exoskeleton is realized through an impedance controller. Ground contacts are also included in the stack of tasks. Models and control were evaluated using the determination coefficient (R^2) method. The pathological gait was modeled with a (R^2) > 99%, control of the exoskeleton alone with a (R^2) > 99%, control of the human inside the exoskeleton with a (R^2) > ..%.**

I. Introduction

A. Context

Exoskeletons are becoming more and more used for the rehabilitation of subjects to help them recover from health issues. Stroke is one of the most common pathologies, with an incidence of 2.0 to 2.5 per 1000 live births, due to stroke cerebral palsy (CP). CP is defined as a "group of non-progressive, but often changing, motor impairment syndromes secondary to lesions or anomalies of the brain arising in the early stages of development" [1]. CP can be provoked by issues with genes, malformations during the conception of the child, cerebral hypoxia around the birth, or prematurity. The severity of the CP can be quantified using different tools. One of them is the Growth Motor Function Classification System (GMFCS) decomposed in 5 levels, from the lowest severity to the highest. Among all the subtypes of CP, the spastic subtype is one of the most studied in the literature. In [2] and [3], it is defined as the most common disabling condition seen in cerebral palsy. Spasticity is a condition in which there is an abnormal increase in muscle tone which might interfere with movement and gait. It creates pathological and involuntary reflexes as explained in [4] and [5]. Spasticity is also known to be a "hypersensitive, velocity-dependent response to passive muscle stretch" [6],[7]: when the movement is too quick, spasticity will have a huge effect on the movement. In this paper we will focus on modeling and control of the kinematics of a 9 years old girl called C, who has CP with a GMFCS level of 2. In particular, we will focus on the interaction between the human (C) and an exoskeleton. The data used will be based on experiments performed on two 9 years old twin sisters, one with spastic cerebral palsy (C) and a healthy one (H) without any impairments. Data from H is used as reference for the behaviour of the exoskeleton. The control of the exoskeleton will be done using a Weighted Quadratic Programming (WQP) library, called Task Space Inverse Dynamics (TSID)[8]. Quadratic Programming (QP) are fast optimization techniques used to solve such nonlinear problems, employing the whole-body kinematics or dynamics of the robot. The goal of this work is to determine if and how an exoskeleton can correct the gait of a child with cerebral palsy. This paper is part of the project to create a customized exoskeleton for a child with a specific spastic cerebral palsy.

B. State of the Art

Several papers focused their work on the control of a human-exoskeleton system as [9]–[12] or [13]. One of the main topic is the interaction model between the human and the exoskeleton. This interaction can be defined as a torque as in [9] . This torque is the stiffness damped torque based on the lower limb human model. Interaction can also be seen as 2 systems in parallel [10] [12]: as human model and the exoskeleton are coupled together, it is assumed they are parallel to each other and the joints angles are equal. These papers described the human motion using transfer functions or raw mechanical equations. The control has been done using an impedance [9] [10] [12] or an admittance controller [11][13]. PID schemes are widely used in the literature to create those controllers as in [10][12].

C. Contribution

This paper used an open-source control framework named Task-Space Inverse Dynamics (TSID) to simulate the control of a lower limb exoskeleton. This software only requires a URDF model of the studied objects, and thus facilitates the definition of the human and exoskeleton systems and their control. The exoskeleton interacts with a human model through torque coupling, and is controlled in impedance. The gaits used during this work are based on real walks from a subject diagnosed with CP.

II. Methods

A. Participants:

Two 9 years old twin sisters (C and H) performed a clinical gait analysis (CGA). C has a GMFCS of 2. Before

[1]Université de Toulouse, CNRS, ICA, ISAE-SUPAERO, Toulouse, France
[2]LAAS-CNRS, Université de Toulouse, CNRS, UPS, France

data collection, we obtained informed consent and assent from the parents and the twin, respectively. The parents also have signed an informed agreement that the Declaration of Helsinki is respected during the experiment. H completed 18 walking trials and C completed 9 walking trials.The anthropometry of C and H were measured: their height, weight, the length of their body segments (Table I). The masses of the segments were computed using regression equations of [14] for children of 9 years old.

Parameter	H	C
Height (cm)	134	123
Body weight (kg)	25	22
Length of the shank (cm)	32	28
Mass of the shank (kg)	1.25	1.1
Mass of the foot (kg)	0.52	0.46

TABLE I

BODY PARAMETERS OF THE TWO TWINS

B. Experimental data acquisition

48 markers were fixed on subject bone landmarks following the recommendation of the International Society of Biomechanics (ISB) [15][16]. The positions of the reflective markers were recorded by twenty optoelectronic cameras sampled at 200 Hz (VICON, Oxford's metrics, Oxford, UK). 6-dimensional external contact wrench applied to the subject by the ground was recorded by five force plates, 2 AMTI platforms and 3 Sensix force platforms, embedded in the ground and sampled at 2 KHz.
Sixteen wireless electromyography (EMG) electrodes were placed on the bodies based on the SENIAM recommendations [17] for both legs. Prior to electrode application, the skin was shaved and cleaned with alcohol. The electrodes were active parallel bar sensors and were placed in the middle of the muscle. Electrodes were secured with adhesive tape before recording. EMG signals were digitized at a 2 KHz sampling rate.

C. Models

Two robots were modeled and used in this paper: one for the Human, and one for the Exoskeleton.

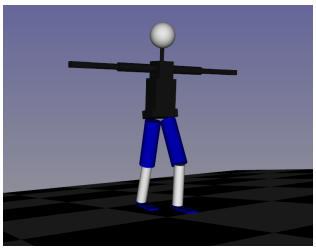

Fig. 1. 48 DOF robot representing the Human

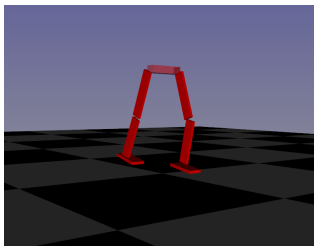

Fig. 2. 12 DOF robot representing the Exoskeleton

1) The "Human": The robot representing the human is a 48 degrees of freedom (DOF) robot with the same anthropometry as C, as shown in Figure 1. Masses, lengths and inertias of all of the links were computed using the information of C presented in Table I and with regression equations from anthropometric tables as [14] and **Dumas**.

2) The "Exoskeleton": The exoskeleton is a 12 degrees of freedom (DOF) robot. Each leg has 6 DOF: 3 DOF at the hip (flexion/extension, adduction/abduction, torsion), 1 DOF at the knee(flexion/extension) and 2 DOF at the ankle (flexion/extension, adduction/abduction). Among these 12 DOF, only 6 joints are actuated: the flexion/extension of the hip, knee, and ankle on each leg. The exoskeleton has the same lengths links as the human, and the joints of the exoskeleton are co-radial. Table II presents all the data about this exoskeleton.

Parameters	Exoskeleton
Material	Steel
Length of the thigh (cm)	33
Mass of the thigh (kg)	0.432
Length of the shank (cm)	28
Mass of the shank (kg)	0.385
Length of the foot (cm)	20
Mass of the foot (kg)	0.21

TABLE II

EXOSKELETON PARAMETERS

D. Task Space Inverse Dynamics (TSID)

Task Space Inverse Dynamics (TSID) is a Weighted Quadratic Program (WQP) [18], commonly used as a control framework for several applications in legged robotics [19] [20] [21]. When given a set of tasks to execute, it computes a whole-body control which respects a hierarchy given to the tasks through weights, priority levels, and gains. TSID has two levels of priorities for now. The level 0 is a set of equalities where, by default there is at least one constraint: the dynamical equation which relates torques and acceleration. Level 1 is solved in the null-space of level 0 and is a multi objective function. Thus when a task is inserted in the stack-of-tasks is has a weight. The weight applied to the task gives its importance: the higher the weight is, the more likely the task will be realized. Finally, K_p and K_d are respectively the proportional and derivative gains used by TSID to impose a dynamic to the task.

Let us consider a second order derivable task-function $x(q)$, where q, the robot configuration vector. and $\dot{q}$, the joint velocity, are the control inputs. The task error e to minimize is defined as:

$$\ddot{e} = \ddot{x}(q) - \ddot{x}(t)^* \tag{1}$$

$$\ddot{e} = (J\ddot{q} + \dot{J}\dot{q}) - \ddot{x}(t)^* \tag{2}$$

with $x(t)^*$ the desired state of the robot, and J its Jacobian.

The correction of the error can be defined as follows :

$$\ddot{e} = K_p(x(q) - x(t)^*) + K_d(\dot{x}(q) - \dot{x}(t)^*) \quad (3)$$

with K_p and K_d, proportional and derivative gains to correct the error in position and velocity. During the rest of this work, K_d is systematically chosen as $K_d = 2\sqrt{K_p}$.

Different tasks are used for each step of this work, as detailed in the next part.

E. Simulations

Two types of simulations were used during this work: simulations of a fixed-base robot, or a free-flyer.

1) Fixed-base: In the first place, the position and orientation of the base of the robot are fixed with regards to its environment. The desired gait is modeled in TSID as a *Posture Task*, and the reference given is chosen among the joint angles trajectories extracted from the experiments, as described in the *Materials* part. The gait was first simulated on the human model, then on the exoskeleton model, then on both at the same time with a torque coupling.

2) Free-flyer: In the second place, the position and orientation of the base is freed, to allow the robot to move in its environment, as happens during a walk. The complexity of the simulation increases as more tasks are required, especially the creation of ground contacts. These contacts are added and removed in accordance with the events identified from the experiments. In these simulations, several tasks are used:

- *Posture Task*: its goal is to produce a gait close to the reference gait extracted from the experiments.
- *CoM Task*: the trajectory of the Center of Mass (CoM) of the robot should remain close to the reference centroidal trajectory. The reference used is computed from the markers data, following the method of the reconstructed pelvis as presented in [22].
- *SE3 Tasks*: an SE3 task takes for reference the desired placement (position and orientation) of a frame. In our case, one SE3 task per foot is created, to ensure the feet trajectory remains close to that extracted from the markers data.

As previously, the free-flyer simulations were first done on the human, then on the exoskeleton, then on both at the same time with torque coupling.

For each simulation, the parameters used will be given along with the simulation results in the next part. The simulations realized in this paper have been made using the Gepetto Viewer software [23] and an Intelő Core i5-8400H CPU @ 2.50GHz Œ 8 processor.

III. Results

A. Recreation of the spastic gait on the human

In this part, the reference gait used for the human control is the "spastic gait" (C).

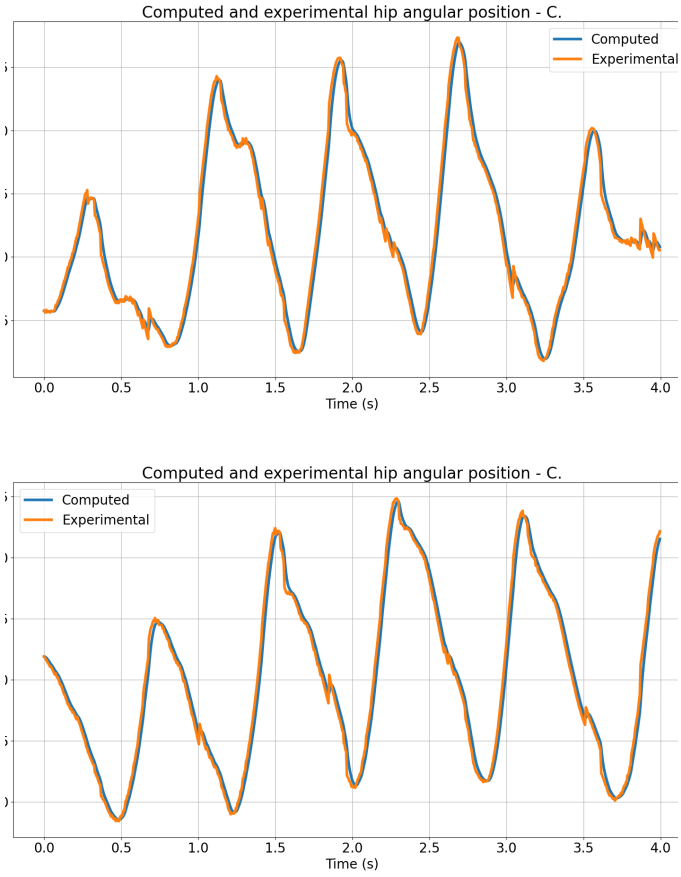

Fig. 3. Computed and experimental data of left (top) and right (bottom) hip during a whole gait in fixed-base

1) Fixed-base: The spastic gait is first modeled as a "Posture Task" using TSID, in a fixed-base simulation, on the human. The parameters used are presented in Table III.

Parameters	Posture
weight	1
priority level)	1
K_p	8e3

TABLE III

Simulation Parameters: human in fixed-base

Results presented in Figure 3 show an example of the efficiency of the WQP which succeeds in creating a corresponding gait behaviour to the reference. The R^2 obtained is around 99% which allows us to affirm that TSID can easily produce a specific gait thanks to the optimization part of it and the inverse dynamics.

2) Free-Flyer: The gait is then recreated in free-flyer. There are two posture tasks: one on the actuated joints (flexion/extension on the hips/knees/ankles), and one on the non-actuated joints. The first one aims at following the experimental gait, while the second one allows for more freedom. Besides the posture tasks, a CoM task is created,

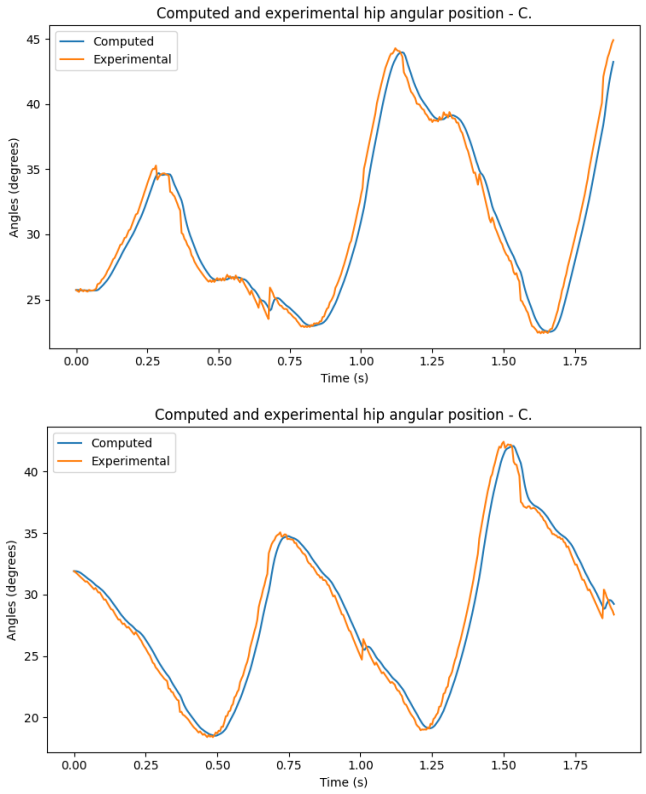

Fig. 4. Computed and experimental data of left (top) and right (bottom) hip during a whole gait with in free-flyer

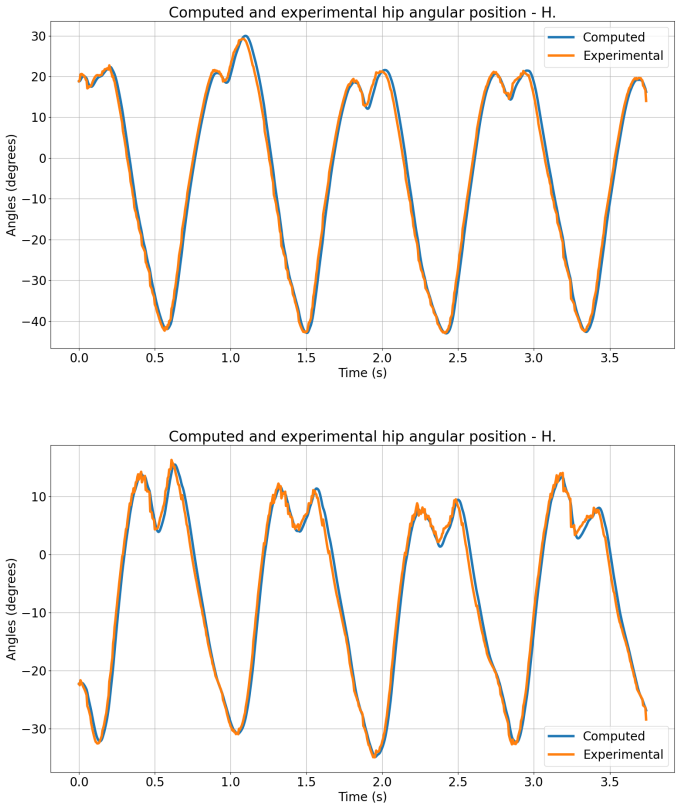

Fig. 5. Computed and experimental model of right joints during a whole walk

along with two SE3 tasks *Right Foot* and *Left Foot*, and contacts between the right foot, the left foot and the floor. The contacts and the SE3 tasks do not coexist: when there is a double support phase, there are two contacts, and no SE3 task. When there is a single support phase, the foot creating the support is in contact with the floor, and there is a SE3 task on the other foot. The parameters used are presented in Table IV.

Parameters	Posture (actuated)	Posture (non-actuated)	CoM	Feet	Contact
weight	1	1e-5	1e-1	1e-1	1e-5
priority level	1	1	1	1	0
K_p	1e4	5e3	1e3	1e4	1e3

TABLE IV
SIMULATION PARAMETERS: HUMAN IN FREE-FLYER

The R^2 obtained is greater than 95% for each joint.

B. Control of the exoskeleton alone

In this part, the reference gait used for the exoskeleton control is the "healthy" walk, so that it can be used later to improve the overall gait in the coupling.

1) Fixed-base: As in the section III-A.1, a Posture Task was created using different parameters in order to fit the gait modeled on the exoskeleton to the reference gait. A "PD+" controller was also added to track the error after the computation of the angular position and velocity of each joints. This PD+ controller is defined as follow :

$$T_{pd+} = P * (q_{tsid} - q_{ref}) + D * (\dot{q_{tsid}} - \dot{q_{ref}}) \quad (4)$$

This torque has been add to the torque computed by TSID and applied to a forward kinematics of the robot in order to obtain the corresponding acceleration to this new torque.
The parameters for TSID and the PD+ are presented in Table V.

Parameters	Posture
weight	1
priority level)	1
K_p	1e4
P	3
D	0.01

TABLE V
SIMULATION PARAMETERS: EXOSKELETON IN FIXED-BASE

As the previous "Posture Task" created, the results here show again that a corresponding gait behaviour to the reference one can be create as shown in Figure 5 for a whole gait. The R^2 obtained is greater than 99% for each joints modeled.

2) Free-Flyer: The gait is also recreated in free-flyer. The same tasks were implemented as for the simulation of the

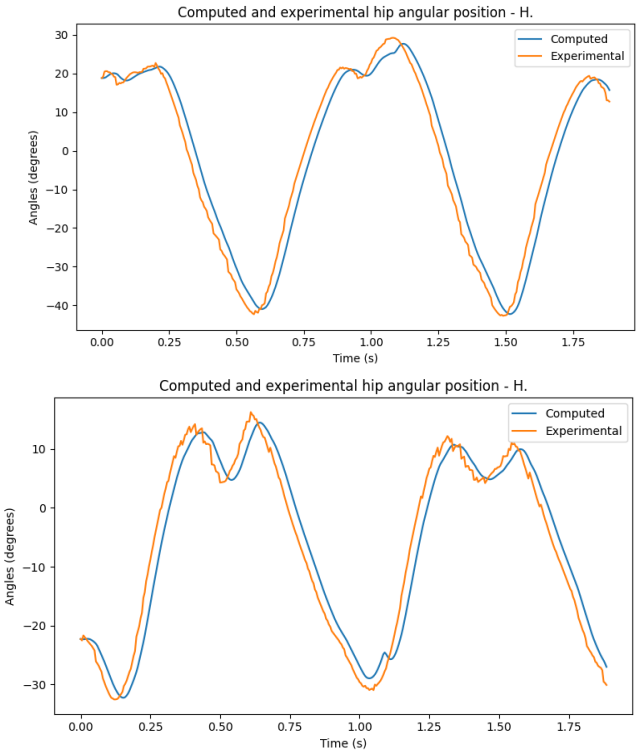

Fig. 6. Computed and experimental data of left (top) and right (bottom) hip during a whole gait with in free-flyer

human walk, but with different parameters presented in Table VI.

Parameters	Posture (actuated)	Posture (non-actuated)	CoM	Feet	Contact
weight	1	1e-3	1	1e-1	1e-5
priority level	1	1	1	1	0
K_p	5e3	3e3	1e3	5e3	1e3

TABLE VI

SIMULATION PARAMETERS: EXOSKELETON IN FREE-FLYER

The R^2 obtained is greater than 94% for both hips, greater than 88% for both knees, but only greater than 76% for the ankles.

The difference between the accuracy of the human and the exoskeleton could be explained by the fact that the human simulated uses its arms to regain balance and stabilise its CoM, while the exoskeleton cannot. In this regard, the coupling between the exoskeleton and the human should improve the accuracy of the gait reproduction

C. Control of the human inside the exoskeleton

This part will present interactions modeled between the human and the exoskeleton as shown in Figure 7. 2 methods of interaction were tested: an imposed gait and a cohabitation gait.

1) Imposed gait by the exoskeleton: Whatever the human can do, the exoskeleton will have the upper hand over the

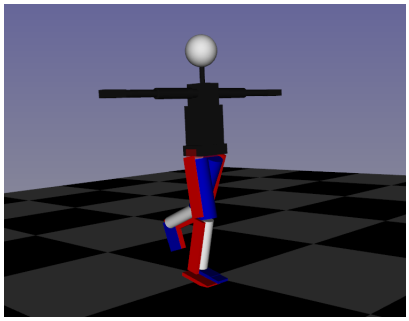

Fig. 7. Simulation of the human inside the exoskeleton

human. It is a "master-slave" interaction and the reference of the exoskeleton is the same as the human. So, the kinematics output of the human and the exoskeleton are the same. This method has been used in [10] and simplifies the interaction between the human and the exoskeleton. Two posture tasks were then defined : one for the exoskeleton and one for the human.

The parameters used are presented in Table VII. The schema

TABLE VII

SIMULATION PARAMETERS

Parameters	Posture human	Posture exo
weight	1	1
priority level)	1	1
K_p	1e4	4e4

of this interaction is represented in Figure **??**. To be done

For this type of control, the results obtained are:

- correspondance between exoskeleton kinematics and the references: $R^2 > 99\%$
- correspondance between human kinematics and the references: $R^2 > 99\%$

This model considers that the human and the exoskeleton have the same goal at each timestep. It can be seen, in real life, as a total control of the exoskeleton over the human. It considers that the human will follow perfectly the exoskeleton which can be the case in the first steps of rehabilitation phase where the movements are imposed.

2) Cohabitation of two behaviors: This model considers that the exoskeleton has its own kinematics references, and so does the human [9]. The interaction is here modelised by a torsion link between each joint of the exoskeleton and the human. The idea is to make the human posture converge to the exoskeleton reference, thanks to this link defined as a torsion torque. The torsion torque $T_{torsion}$ can be defined as:

$$T_{torsion} = S(\Theta_m - \Theta_k) + D(\Theta'_m - \Theta'_k)$$

with:

S and D : gains respectively for the spring and the damper,

Θ_m, Θ_k : angular position of the hip/knee exoskeleton and of the hip/knee of the human,

Θ'_m, Θ'_k : angular velocity of the hip/knee exoskeleton and

of the hip/knee of the human. To be done

3) Adaptation in free-flyer: To be done

IV. Discussions

To be done

TABLE VIII
COEFFICIENTS OF DETERMINATION OBTAINED

Value of (R^2)	Hips	Knees	Ankles
Human (fixed-base)	$> 99\%$	$> 99\%$	$> 99\%$
Human (free-flyer)	$> 95\%$	$> 95\%$	$> 95\%$
Exo (fixed-base)	$> 99\%$	$> 99\%$	$> 99\%$
Exo (free-flyer)	$> 94\%$	$> 88\%$	$> 76\%$
Coupling (fixed-base)			
Coupling (free-flyer)			

Future works will include a human gait model defined using EMG data as those data were not used in this paper. Other methods of control as admittance controller will be tested and compared to this paper.

V. Conclusions

This paper aims to model and control a human inside the exoskeleton using a coupling torque and TSID as a control framework. The final purpose of this study is to realize a customized exoskeleton for a subject with a spastic cerebral palsy.Results demonstrate the efficiency of TSID to create optimal gait cycles based on experimental data obtained from clinical gait analysis.
The "Fixed-base" results ..
The "Free-Flyer" results ...

All of our codes and simulations produced during this work are available at : LIEN GIT.

Acknowledgement

The authors would like to thank the Région Occitanie and Université Fédérale Toulouse Midi-Pyrénées (UFTMIP) for their financial support.

Conflict of interest statement

The authors confirm that there are no conflicts of interests regarding the work described in the current manuscript.

References

[1] P. Rosenbaum, "Cerebral palsy: What parents and doctors want to know," *BMJ (Clinical research ed.),*, vol. 326(7396), pp. 970–974. 2003. DOI: 10.1136/bmj.326.7396.970.

[2] H. K. Graham, "Pendulum test in cerebral palsy," *Lancet (London, England)*, vol. 355(9222), p. 2184, 2000. DOI: 10.1016/s0140-6736(00)02399-0.

[3] P. O. Pharoah, T. Cooke, I. Rosenbloom, and R. W. Cooke, "Trends in birth prevalence of cerebral palsy.," *Archives of disease in childhood*, vol. 62(4), pp. 379–384, 1987. DOI: 10.1136/adc.62.4.379.

[4] J. W. Lance, "What is spasticity?" *Lancet (London, England)*, vol. 335(8689), pp. 108–115, 1990. DOI: 10.1016/0140-6736(90)90389-m.

[5] A. Kheder and K. P. Nair, "Spasticity: Pathophysiology, evaluation and management," *Practical neurology*, vol. 12(5), pp. 289–298, 2012. DOI: 10.1136/practneurol-2011-000155.

[6] J. W. J. Fee and R. A. Foulds, "Neuromuscular modeling of spasticity in cerebral palsy," *IEEE transactions on neural systems and rehabilitation engineering : a publication of the IEEE Engineering in Medicine and Biology Society*, vol. 12(1), pp. 55–64, 2004. DOI: 10.1109/TNSRE.2003.819926.

[7] M. R. Dimitrijevic, "Spasticity," *Scientific Basis of Clinical Neurology*, pp. 108–115, 1985.

[8] ——, "Tsid," [Online]. Available: https://github.com/stack-of-tasks/tsid.

[9] Y. Huo, X. Li, X. Zhang, and D. Sun, "Intention-driven variable impedance control for physical human-robot interaction," in *2021 IEEE/ASME International Conference on Advanced Intelligent Mechatronics (AIM)*, IEEE, 2021, pp. 1220–1225.

[10] M. S. Amiri, R. B. Ramli, M. F. Ibrahim, D. A. Wahab, and N. K. Aliman, "Adaptive particle swarm optimization of pid gain tuning for lower-limb human exoskeleton in virtual environment," 2020.

[11] A. del-Ama, Á. Gil-Agudo, and J. e. a. Pons, "Hybrid fes-robot cooperative control of ambulatory gait rehabilitation exoskeleton," 2014. DOI: 10.1186/1743-0003-11-27.

[12] Z. F. Lerner, D. L. Damiano, H.-S. Park, A. J. Gravunder, and T. C. Bulea, "A robotic exoskeleton for treatment of crouch gait in children with cerebral palsy: Design and initial application," *IEEE Transactions on Neural Systems and Rehabilitation Engineering*, vol. 25, no. 6, pp. 650–659, 2017. DOI: 10.1109/TNSRE.2016.2595501.

[13] Y. Tu, A. Zhu, J. Song, *et al.*, "An adaptive sliding mode variable admittance control method for lower limb rehabilitation exoskeleton robot," *Applied Sciences*, vol. 10, p. 2536, Apr. 2020. DOI: 10.3390/app10072536.

[14] R. K. Jensen, "Body segment mass, radius and radius of gyration proportions of children," *Journal of biomechanics*, vol. 19(5), pp. 359–368, 1986. DOI: 10.1016/0021-9290(86)90.

[15] G. Wu, S. Siegler, P. Allard, C. Kirtley, A. Leardini, and D. Rosenbaum, "Isb recommendation on denitions of joint coordinate system of various joints for the reporting of human joint motion-part i: Ankle, hip, and spine.," *J.Biomech*, vol. 35(4):543-8, 2002.

[16] G. Wu, "Isb recommendation on denitions of joint coordinate systems of various joints for the reporting of human joint motionpart ii: Shoulder, elbow, wrist and hand.," *J.Biomech*, vol. 38(5):981, 2005.

[17] H. J. Hermens, B. Freriks, C. Disselhorst-Klug, and G. Rau, "Development of recommendations for semg

sensors and sensor placement procedures. journal of electromyography and kinesiology," *International Society of Electrophysiological Kinesiology*, vol. 10(5), pp. 361–374, 2000. DOI: 10.1016/s1050-6411(00)00027-4.

[18] A. Del Prete, N. Mansard, O. E. Ramos, O. Stasse, and F. Nori, "Implementing torque control with high-ratio gear boxes and without joint-torque sensors," in *Int. Journal of Humanoid Robotics*, 2016, p. 1 550 044. [Online]. Available: https://hal.archives-ouvertes.fr/hal-01136936/document.

[19] N. Ramuzat, G. Buondonno, S. Boria, and O. Stasse, "Comparison of Position and Torque Whole Body Control Schemes on the Humanoid Robot TALOS," in *20th International Conference on Advanced Robotics (ICAR)*, Virtual event, Slovenia, Dec. 2021. DOI: 10.1109/ICAR53236.2021.9659380. [Online]. Available: https://hal.archives-ouvertes.fr/hal-03145141.

[20] T. Corbères, T. Flayols, P.-A. Léziart, *et al.*, "Comparison of predictive controllers for locomotion and balance recovery of quadruped robots," in *IEEE International Conference on Robotics and Automation (ICRA 2021)*, Xi'an, China, May 2021. DOI: 10.1109/ICRA48506.2021.9560976. [Online]. Available: https://hal.laas.fr/hal-03034022.

[21] M. Boukheddimi, F. Bailly, P. Souères, and B. Watier, "Human-like gait generation from a reduced set of tasks using the hierarchical control framework from robotics," in *IEEE International Conference on Robotics and Biomimetics (ROBIO 2019)*, ser. IEEE International Conference on Robotics and Biomimetics (ROBIO 2019), Dali, China: IEEE, Dec. 2019, pp. 2683–2688. DOI: 10.1109/ROBIO49542.2019.8961426. [Online]. Available: https://hal.archives-ouvertes.fr/hal-02455162.

[22] M. Saini, D. C. Kerrigan, M. A. Thirunarayan, and M. Duff-Raffaele, "The vertical displacement of the center of mass during walking: A comparison of four measurement methods," 1, vol. 120, 1998, pp. 133–139.

[23] LAAS-CNRS, J. Carpentier, and M. Geisert, *Gepetto-viewer*, version 4.13.0, May 31, 2022. [Online]. Available: https://github.com/Gepetto/gepetto-viewer.